





REGULAR PAPER

# A practical design approach for a single-stage sounding rocket to reach a target altitude

J. Huh<sup>1,2,\*</sup>  and S. Kwon<sup>3</sup> 

<sup>1</sup>Department of Mechanical and Aerospace Engineering, College of Engineering, United Arab Emirates University, P.O. Box 15551, Al Ain, Abu Dhabi, United Arab Emirates, <sup>2</sup>National Space Science and Technology Center (NSSTC), United Arab Emirates University, P.O. Box 15551, Al Ain, Abu Dhabi, United Arab Emirates and <sup>3</sup>Department of Aerospace Engineering, Korea Advanced Institute of Science and Technology (KAIST), 291 Daehak-ro, Yuseong-gu, Daejeon, 34141, Republic of Korea

\*Corresponding author: Email: [j.huh@uaeu.ac.ae](mailto:j.huh@uaeu.ac.ae)

**Received:** 6 September 2021; **Revised:** 21 January 2022; **Accepted:** 24 January 2022

**Keywords:** Sounding rocket; Design practicality; Design methodology; Reachable altitude; Flight optimisation

## Abstract

A new type of design domain for a sounding rocket is suggested in this study, which is more intuitive, simplified, and conducive to a single-stage sounding rocket development process. Among the various operation parameters, this study identifies several effective variables, which are also among the most practical in a sounding rocket design process. Of the many design variables considered for peak altitude optimisation, arguably the three most effective in shaping the whole system and conferring the most practicality in the design process of a sounding rocket were determined. A simulation-based study was conducted to establish: the effect of the selected parameters on flight performance, and the optimum design conditions of a single-stage sounding rocket in terms of its peak altitude. The simulation result was compared with randomly chosen experimentally tested flight data and validated. With the clear performance curves varying depending on the variables, the combination of the considered design inputs was effective. The new type of design domain and design procedure proposed is expected to constitute a useful reference and deliver practical benefits to the development process for a target-altitude-optimised single-stage sounding rocket.

## Nomenclature

$C_d$	drag coefficient
$C_{dy}$	side drag coefficient
$C_l$	lift coefficient
$D$	drag force [N]
$D_y$	side drag force [N]
$F$	net force [N]
$F_b$	aerodynamics force [N]
$F_g$	gravitational force [N]
$F_t$	thrust force [N]
$g$	gravitational acceleration [ $\text{m/s}^2$ ]
$g_0$	gravitational acceleration at sea level [ $\text{m/s}^2$ ]
$H$	angular momentum [ $\text{kg}\cdot\text{m}^2/\text{s}$ ]
$I_{sp}$	specific impulse [s]
$k$	specific heat ratio
$L$	lift force [N]
$m$	flight vehicle mass [kg]
$m_0$	rocket initial mass [kg]
$m_p$	rocket propellant mass [kg]

$M$	net torque [N-m]
$MR$	mass ratio
$p$	angular velocity for roll axis [rad/s]
$P_c$	chamber pressure [Pa]
$P_e$	ambient pressure [Pa]
$q$	angular velocity for pitch axis [rad/s]
$r$	angular velocity for yaw axis [rad/s]
$R$	gas constant [J/(kg-K)]
$S$	cross sectional area in axial direction [m <sup>2</sup> ]
$S_y$	cross sectional area in transverse direction [m <sup>2</sup> ]
$T$	magnitude of thrust [N]
$T_c$	chamber temperature [K]
$v_e$	effective exhaust velocity [m/s]
$\vec{V}$	velocity vector with respect to the inertial frame [m/s]
$V_t$	total velocity of the body fixed frame [m/s]
$\vec{\omega}$	relative angular velocity vector between the body fixed frame and the inertial frame [rad/s]
$x_{cp}$	static margin [m]
$\alpha$	angle of attack [degree]
$\beta$	angle of side slip [degree]
$\zeta$	propellant fraction
$\Theta$	Euler angle for pitch axis [rad]
$\rho$	air density [kg/m <sup>3</sup> ]
$\varphi$	Euler angle for roll axis [rad]
$\psi$	Euler angle for yaw axis [rad]

## 1.0 Introduction

Sounding rockets have been used since the middle of the 20<sup>th</sup> century, and their mission profile for scientific and technological tests has been diverse, in particular during sub-orbital flights. There is now greater demand for sounding rockets, especially at an altitude range of 50 to 100 km, which is too high for scientific balloons due to the low air density at such an altitude, and too low for satellites due to their large drag and limited operational capacity at a low orbit. Today, experimental missions involving sounding rockets are undertaken not only to gain knowledge of space system integration and flight testing itself, but also in regard to the mandatory atmosphere inspections requested by the UN, scientific tests in micro gravity near the apogee, single/multi-stage-to-orbit missions, supersonic combustion tests, as well as aerodynamic tests [1–5]. As reaching a certain altitude is crucial to a sounding rocket's operations, which provides test environments with micro gravity, low air density, and sufficient descending velocity with an adequate flight time, the final altitude is one of the most critical parameters of such a rocket's performance and is among the principal design objectives. Not only from this perspective, but also concerning operational efficiency, in light of a new aspect of cost-sensitive space technology emerging recently represented by such as low-cost and reusable launch vehicles [6–12], there is a greater need today for the maximisation of final altitudes and the minimisation of propellant masses of vertically launched flight vehicles.

Arguably the first reported effort to maximise the peak altitude of an ascending rocket took place in 1919 in an analytical approach by R. Goddard [13], at a time when optimisation was linked to additional constraints such as limited flight time, drag-law modelling, dynamic pressure limitations, and thrust constraints [14–17]. Further studies then followed demonstrating potential optimisation conditions for an optimum peak altitude. The issue of altitude optimisation was first approached from an analytical point of view based on mathematical solutions, before simulation-based studies [18] followed demonstrating more optimised flight conditions. Both approaches have informed guidelines on the flight conditions of vehicles and have been beneficial, regardless of whether it is physically possible to meet the theoretical requirements or not. In fact, the outcomes from these studies are examples of theoretical

optimisation, and there was a lack of sufficient interest in ascertaining how to practically achieve the optimised conditions from a flight vehicle design point of view in order to reach a target altitude.

Thus, certain design variables or flight performance parameters considered in the previous research were more useful for theoretical performance estimations and/or the optimisation process than in the design process of a rocket. For example, the thrust curve programming, with the magnitude of thrust variation during operation under the constraint of flight time [14], which attracted lots of interest in previous studies [13–17] attempting to maximise the final altitude of vertically ascending rockets, do not represent the most practically effective parameters and baselines for a sounding rocket design and its system configuration procedure. In fact, little research on the maximisation of the final altitude focused on this. However, selecting appropriate design variables and applying them to an altitude optimisation process is essential to make those optimised conditions physically feasible and effective in regard to the design process.

In this work, therefore, considerable effort was made to determine those variables that are most effective and practical in a sounding rocket design and the optimisation process. This study will also attempt to distinguish itself from previous research which focused on theoretical optimisation and whose assumptions were relevant to mathematical models but lacking sufficient contemplation of the practical considerations. Flight performance data was acquired in flight simulations via a shooting method, which was conducted using an in-house code flight simulator. The simulation results were analysed to understand the effects of the selected parameters on flight performance, and a new type of design domain with an optimised design reference was provided. The reachable altitude performance estimated through the simulation work was also compared with other experimental based studies for validation, and previous findings, such as the optimum initial acceleration for the maximisation of peak altitude, were also verified demonstrating its consistency. Finally, utilising the design domain provided, a simplified and intuitive design procedure (three-variable design method) has been proposed for a single-stage sounding rocket from a practical design point of view to reach the optimised target altitude.

## 2.0 Maximisation of a final altitude of an ascending rocket: the Goddard problem

The problem of maximising a final altitude of a vertically launched rocket can be traced back to 1919 when Robert H. Goddard [13] attempted to find the optimum thrust curve for a given amount of propellant. The eponymous Goddard problem was approached using different mathematical methods, including the calculus of variations at an earlier time and a few assumptions on the equations of motion, circumventing difficulties in solving the governing equation analytically, before more constraints were considered later, followed by numerical analysis and optimal control theory studies. The problem has been addressed extensively with reference to additional constraints such as constrained time of flight [14], a drag-law and its effects [15], a dynamic pressure limitation [16], bounded thrust [19], and both dynamic pressure and thrust constraints [17].

Goddard [13] proposed the problem of maximising the altitude of a rocket in a vertical flight with a given amount of propellant, which was akin to minimising the required propellant mass to transfer a rocket to an assigned maximal height, finding an optimised thrust composed of a piecewise continuous thrust function of time. He identified the problem as an unsolved problem of the calculus of variations and suggested no further formulation or solution. A few years later, Hamel [20] proved the existence of a solution by means of the calculations of variations, with an assumption of a linear rocket mass variation. More assumptions were considered in the following studies on the Goddard problem.

Malina et al. [21] considered a rocket launched vertically in a vacuum and in a resisting medium condition. In order to show maximum height as a function of three variables they mainly explored: effective exhaust velocity, mass ratio, and initial acceleration. They discovered that without consideration of an aerodynamics drag force, it is best to use the propellant in the shortest possible time reaching maximum velocity immediately, based on a numerically estimated reachable altitude that increased with increasing initial acceleration. However, with an aerodynamics drag, high initial velocity had a negative

impact on peak altitude maximisation due to the high aerodynamics drag that tends to occur at a low altitude, where the air is relatively denser than that of a higher altitude. Thus, in such cases, a prolonged powered-flight was beneficial to get over the hump of the drag curve, allowing a rocket to reach a higher altitude. In other words, there was a certain initial acceleration that is optimal for a maximum altitude, which was later found again by Ivey et al. [22], with a range of one to three times gravitational acceleration.

Tsien et al. [23] provided an extensive numerical analysis of flight trajectories to show optimum thrust programming by considering a velocity dependent linear drag and a quadratic drag. With a varying drag model, it was found that it is more advantageous to have a lower velocity at low altitudes in order to increase the altitude at the end of the propellant burning cycle. For the optimum thrust programming, after the initial impulse, the amount of thrust should increase with altitude in general. In addition, as the linear drag does not increase with velocity as quickly as the quadratic drag, the linear drag favours a shorter burn time and high velocity with large initial acceleration to obtain a higher reachable altitude, while the drag from the quadratic model favours lower velocity and longer burn time.

Bryson Jr et al. [24] devised a method to handle a non-increasing rocket mass constraint and some numerical calculations, resulting in optimum trajectories that took into account an aerodynamic drag. During its three flight stages, composed of an initial instantaneous boost, a sustain phase, and a coasting phase, the optimised initial flight path angle was 69 degrees ground-to-ground for the maximum range, the value of which would have been 45 degrees in the absence of drag. The study examined the difference between trajectories with an aerodynamic drag and without.

Garfinkel [25] tried to broaden the number of soluble cases rather than focusing on a select few specific ones allowing previous solutions to meet the monotone rocket mass requirement, which had caused the problem at that time. The study solved the thrust optimising problem of a vertically ascending rocket, assuming an isothermal atmosphere and admissibility of an infinite thruster, in two specific cases: 1) Mach number and fuel supply are sufficiently large, and 2) the drag is a convex function of velocity. The first scenario embraced very general physical drag functions and was valid for Earth, while the second was extended to all atmospheric conditions including extra-terrestrial with limited applicability to drag functions, which was reasonably common at that time, in order to make the Goddard problem solvable.

Munick [19] considered a bounded thrust, identifying an optimised thrust programming that consisted of a piecewise continuous thrust as a function of time to maximise its peak altitude. It was concluded that when using the thrust sufficiently high in a finite level, the optimal control contains three subarc functions at most. The results of Munick's research extended the findings of previous studies to a larger range of drag functions, including a drag range near the speed of sound.

Seywald's study [16,26] was concerned with the effect of two additional conditions as constraints: a dynamics pressure limit and a specified final time. The effect of those restrictions on an optimal thrust switching structure was investigated and a thrust structure was identified for a maximum attainable altitude using nine different types of thrust arcs. The constrained time of flight was also one of the conditions considered for the Goddard problem and the maximisation of altitude and for a given flight time in Panagiotis's study [14] where maximising the final altitude of a vertically launched rockets has been analysed in regard to quadratic draw law and bounded thrust. Seywald's work was then further explored by Graichen and Petit [17] concerning dynamics pressure and thrust constraints using a different methodology. By using a saturation function, it systematically incorporated the constraints into the equation and resulted in an unconstrained optimal control problem that required no knowledge of the thrust switching structure, implying its broader applicability to various constraints.

All of these efforts, which have continued until the last decade, have largely focused on the shape of the aerodynamic drag function, considering it one of the major concerns in terms of making the equation of motion more accommodating when approaching the Goddard problem. There has also been an interest in additional constraints for optimisation, including dynamic pressure limitation, atmospheric density, a limited time of flight, thrust constraints, and optimum thrust programming, implying several

assumptions were beneficial in regard to the mathematical models and methods adopted in the previous theoretical studies. The results from the theoretical work on optimum conditions represent a useful guide for rocket operational conditions in that they detail the influence of several design and operational parameters on rocket flight performance. However, although the preliminary analysis is informative, to some extent, in designing a rocket, it does not necessarily guarantee that the operational conditions suggested are physically feasible, as the analysis was approached mathematically with less emphasis on the practicability of the system configuration from a rocket design point of view. Therefore, in relation to optimal flight, further research on design parameters is required with a greater emphasis on their practical properties which are conducive to peak altitude maximisation. This is the main concern and objective of this work, which will propose a new design approach along such lines, detailed in the following sections.

### 3.0 New design approach to altitude maximisation

With regards to an operational design conducive to altitude maximisation, numerous analytical estimation studies and simulation-based approaches have considered the governing equation of motion, producing a range of results. There were several assumptions as to how the analytic equations could be solved, but with limited practicality in real rocket design applications. Simulation-based studies also suggested certain optimisation conditions, but these are arguably too specific to be applied to other rocket designs, and even if a broader range of design variables were considered, they could not be applied pragmatically to an effective rocket design process. Thus, whether the selected design parameters are appropriate determines whether or not the optimisation results are practically applicable to a sounding rocket design process. Despite the numerous variables previously reported, there is also room for more intuitive data on design inputs and their effect on optimised flight performance. More studies are required on this perspective to obtain clearer outputs versus rocket system design inputs (i.e. reachable altitudes optimised with respect to the main rocket design variables).

The principal design parameters of a sounding rocket should be properly determined and considered in optimisation work, not only to provide intuitive and broad rocket design domains which optimise peak altitude, but also to make the optimisation data meaningful in terms of practicability. Thus, considerable effort was made in this work to find both useful, effective and viable design parameters which provided an optimised design domain reference in the design of a sounding rocket, particularly a single staged type.

In reality, as most engines are developed with a certain amount of targeted thrust, while some are available off-the-shelf with certain performance specifications, the magnitude of thrust is one of the most practical design parameters, and it must be considered in the sounding rocket design process. Engine selection or development is generally followed by a system design process that includes a system configuration in relation to pipelines, tanks, valves, casing, payload and electrical systems for avionics, data collection and communication. In terms of practicality, therefore, a burn time is determined by choosing a type of tank and volume which depends on total propellant mass and the maximum combustion duration. Then the mass ratio of the propellant and the rest of the rocket system (dry mass) can be estimated. Thus, primary major design parameters for rocket systems should include a magnitude of thrust, propellant type, burn time and propellant fraction (i.e. mass ratio).

Some might argue that more concern should be accorded to chamber pressure, specific impulse, and propellant flow rate, the importance of which might appear to have been neglected in this study. However, these variables are related to each other and they were considered as dependent variables in this work. For example, following the thrust equation as shown in Equation (1), once the amount of thrust has been determined, the required propellant consumption rate can be calculated considering specific impulse performance.

$$T = \dot{m}_p I_{sp} g_0 \quad (1)$$

$T$  is the magnitude of thrust,  $\dot{m}_p$  propellant mass flow rate,  $I_{sp}$  specific impulse and  $g_0$  gravitational acceleration at sea level. Specific impulse ( $I_{sp}$ ) performance is, as shown in Equation (2), a function of propellant type (specific heat, gas constant and combustion temperature) and working pressure ratio.

$$I_{sp} = \frac{v_e}{g_0} \sim \frac{1}{g_0} \sqrt{\frac{2k}{k-1} RT_c \left[ 1 - \left( \frac{P_e}{P_c} \right)^{(k-1)/k} \right]} \quad (2)$$

$v_e$  is the effective exhaust velocity,  $g_0$  gravitational acceleration at sea level,  $k$  specific heat ratio,  $R$  gas constant,  $T_c$  chamber temperature,  $P_c$  chamber pressure and  $P_e$  ambient pressure. As there is a common range of design values for chamber pressure ( $P_c$ ) to be achieved in a rocket chamber, once propellant type (and thus its specific heat ratio, gas constant, and theoretical combustion temperature, from a chemical equilibrium analysis) is decided, accordingly specific impulse is expected to be in a certain range, and it can be assumed to be determined by propellant type. This is also a reasonable assumption because the chamber pressure effect on specific impulse is not linear. Once the operation chamber pressure reaches a certain amount, its further effect on specific impulse becomes marginal, as seen in Equation (2) for  $I_{sp}$  with respect to the  $P_c$ . Typically, chamber pressure of 20 – 30 bar or more [5,27–30] is considered depending on the mission, but it is typically in the range of several tens of bars for the general chamber design pressure of sounding rockets. Therefore, it is arguably reasonable to assume that specific impulse performance is determined by propellant type. Also, given the potentially limited range of those parameters, they were not the major independent variables considered in this study.

Another aspect making this effective design variables selection more meaningful is that there is a trend in engineering toward sounding rocket sizing, depending on the amount of thrust. For example, as can be seen in the specifications of sounding rockets from previous studies in Table 1, and thrusts and body diameters from single-stage sounding rockets in Fig. 1, despite the differences between the propellant types used, there is a link between sounding rocket body diameter size and the amount of thrust targeted. With regards to this physical aspect of engineering, a flight simulation can be simplified, at least with respect to a drag force, which is proportional to the cross section area of a rocket body. On the basis of this empirical data, the drag force was determined, according to the magnitude of thrust produced by a sounding rocket.

As a result, among the numerous design variables that can be examined as input variables, this study identified three main design parameters which can be applied to a sounding rocket design process with a focus on reachable altitude maximisation: Magnitude of thrust, burn time, and propellant fraction (i.e. mass ratio). The usefulness and/or effectiveness of the selected input variables were expected to be verified in this study, resulting in a new type of design domain with broad and intuitive flight performance characteristics which would represent a design reference for a sounding rocket to reach a target altitude.

#### 4.0 Flight trajectory simulation

In order to investigate the influence of the selected design variables on flight performance and suggest appropriate design domains, a flight trajectory was simulated. A six-degree-of-freedom flight trajectory in-house code was developed and a shooting method was employed. The shooting method is a method used in numerical analysis to find a solution trying different initial conditions until a satisfactory result is obtained. The method was evaluated as suitable for this simulation, as during the solving process it would plot a simulation result for each initial condition, providing a design domain with an optimised design reference.

For the trajectory calculation, the equation of rotational motion, kinematic relation and Newton's second law of motion were considered as the main governing equations. Additionally, the quaternion equation was utilised to circumvent a singular point while solving Euler angles. As Newton's equation of motion applies to an inertial frame, two frames were used; body fixed frame and Earth fixed frame. The body fixed frame was a frame fixed to a rocket, more specifically on the point of the body where the centre of gravity was located, which moves and rotates together with the rocket body during a translational and

**Table 1.** Sounding rocket specifications from previous studies

No	Research group/Model (ref)	Propellant	Thrust [N]	Diameter [cm]	Length [m]
1	DLR HEROS 3 [31]	N <sub>2</sub> O/Paraffin	10,000	22.3	7.5
2	Purdue Univ. GEN-I-R [32]	Solid(M1900 BB)	1,914	15.2	4.7
3	Purdue Univ. GEN-I-F [32]	H <sub>2</sub> O <sub>2</sub> /LDPE	3,115	15.2	4.8
4	Purdue Univ. GEN-II-F [33]	H <sub>2</sub> O <sub>2</sub> /LDPE	3,560	19.1	4.8
5	Warsaw Institute of Aviation ILR-33 [34]	H <sub>2</sub> O <sub>2</sub> /PE	4,000	23	5.0
6	Warsaw Institute of Aviation Amelia 1 [35]	Solid	–	7.3	1.6
7	Warsaw Institute of Aviation Amelia 2 [35]	Solid	700	9.4	2.2
8	Warsaw Institute of Aviation H1 [36]	Solid	–	10	2.1
9	Rocket lab Atea 1 [34]	N <sub>2</sub> O/Polymer	6,700	15	6.0
10	Hokkaido Univ CAMUI 400kgf [37]	LO <sub>x</sub> /PE	4,000	24	–
11	NAMMO Nucleus [38]	H <sub>2</sub> O <sub>2</sub> /HTPB	30,000	35.6	9.0
12	KAIST 250 N [27]	H <sub>2</sub> O <sub>2</sub> /HDPE	250	11	1.1
13	KAIST 1,000 N [39]	H <sub>2</sub> O <sub>2</sub> /HDPE	1,000	15.3	2.4
14	KAIST 2,500 N [-]	H <sub>2</sub> O <sub>2</sub> /HDPE	2,500	20.4	3.4
15	UCLA HyPE 1B2 [40]	N <sub>2</sub> O/Paraffin-HTPB	3,885	20.3	3.9
16	TU Delft Stratos III [41]	N <sub>2</sub> O/Sorbitol-Paraffin-Al	15,000	28	8.2
17	TU Delft Stratos IV [42]	N <sub>2</sub> O/Sorbitol-Paraffin-Al	26,000	28	8.3
18	TU Delft Stratos II+ [42]	N <sub>2</sub> O/Sorbitol-Paraffin-Al	8,000	20	7.0
19	TU Delft Aether [42]	Solid	5,200	21	3.4
20	CNET Belier I [43]	Solid	20,000	31	4.0
21	CNET Belier II [43]	Solid	21,500	31	5.9
22	CNET Belier III [43]	Solid	20,000	31	3.8
23	U KwaZulu-Natal Phoenix-1B MK II [44]	N <sub>2</sub> O/paraffin/AL	7,250	17	4.9
24	U KwaZulu-Natal - [45]	–	2,500	20	4.0
25	U Waterloo Unexploded Ordnance [46]	N <sub>2</sub> O/HTPB/Al	3,358	15.2	4.5
26	Lockheed Martin - [47]	N <sub>2</sub> O/HTPB	6,227	–	–
27	Aerojet Aerobee [48]	Solid	18,000	38.0	7.8
28	U Michigan Laika [49]	N <sub>2</sub> O/Ethanol	3,780	16.3	3.3

rotational motion, and thus it was not an inertial frame. For the Earth fixed frame, North-East-Down (NED) frame was used, which was located at the surface of the Earth and assumed as an inertial frame without consideration of revolution and rotation of the Earth.

For a translational motion, as shown in Equation (3), Newton’s second law of motion was applied to the inertial frame and then expressed with a velocity of the body fixed frame,  $\left(\frac{d\vec{V}}{dt}\right)_r$ , and relative angular velocity between the body fixed and the Earth fixed frame,  $\vec{\omega}$ , where  $m$  is a rocket mass and  $t$  is time.

$$\sum \vec{F} = m \frac{d}{dt} (\vec{V}) = m \left[ \left( \frac{d\vec{V}}{dt} \right)_r + \vec{\omega} \times \vec{V} \right] \tag{3}$$

Thrust, aerodynamic force and gravitational force were taken into consideration for the net force,  $\Sigma \vec{F}$ . Aerodynamic force at the body fixed frame for each axis was, as shown in Equation (4), a function of angle of attack  $\alpha$ , side slip  $\rho$ , air density  $\rho$ , total velocity  $V_t$ , drag coefficient  $C_d$  and  $C_{dy}$ , lift coefficient  $C_l$ , and cross section area  $S$  and  $S_y$ .

$$\vec{F}_b = \begin{bmatrix} F_{bx} \\ F_{by} \\ F_{bz} \end{bmatrix} = \begin{bmatrix} -D \cos \alpha + L \sin \alpha \\ D_y \\ -D \sin \alpha - L \cos \alpha \end{bmatrix} \tag{4}$$

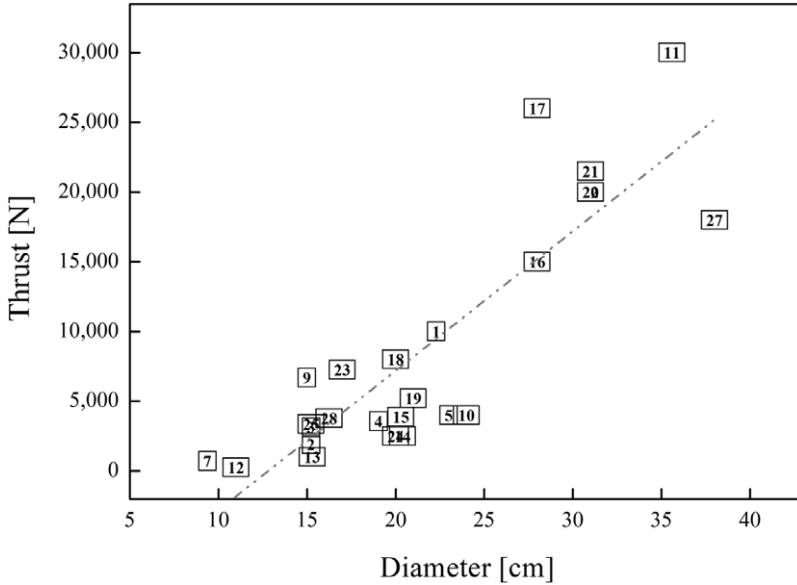


Figure 1. Thrusts and body diameters mainly of single-stage sounding rockets reported in previous studies (from Table 1).

where

$$D = \frac{1}{2} \rho (V_t \cos \beta)^2 S C_d \tag{5}$$

$$L = \frac{1}{2} \rho (V_t \cos \beta)^2 S C_l \tag{6}$$

$$D_y = \frac{1}{2} \rho (V_t \sin \beta)^2 S_y C_{dy} \tag{7}$$

For gravitational force, Euler angles,  $\Psi$ ,  $\theta$ , and  $\varphi$ , were required to identify the rocket attitude and determine the gravitational force distribution to each axis,  $mg_x$ ,  $mg_y$ , and  $mg_z$ .

$$\vec{F}_g = m \vec{g} = m \begin{bmatrix} g_x \\ g_y \\ g_z \end{bmatrix} = \varphi^{-1} \theta^{-1} \begin{bmatrix} 0 \\ 0 \\ mg \end{bmatrix} = \begin{bmatrix} -mg \sin \theta \\ mg \cos \theta \sin \varphi \\ mg \cos \theta \cos \varphi \end{bmatrix} \tag{8}$$

Thrust was assumed to be produced in the axial direction only without consideration of thrust vector control as described in Equation (9).

$$\vec{F}_t = \begin{bmatrix} F_{tx} \\ F_{ty} \\ F_{tz} \end{bmatrix} = \begin{bmatrix} thrust \\ 0 \\ 0 \end{bmatrix} \tag{9}$$

Then Equation (3) for Newton’s second law gave information on the body fixed accelerations  $(\dot{u}, \dot{v}, \dot{w})$ , with the input of aerodynamic force, thrust, gravitational force, mass, velocities  $(u, v, w)$  and angular velocities for each axis  $(p, q, r)$ . Likewise, the rotation motion was calculated by solving the equation of Newton’s second law of rotation, as shown in Equation (10) with inputs of rocket moment of inertias, torques, and angular velocities, for outputs of angular accelerations.

$$\sum \vec{M} = \frac{d\vec{H}}{dt} = \left( \frac{d\vec{H}}{dt} \right)_r + \vec{\omega} \times \vec{H} \tag{10}$$



Torque on each axis ( $\bar{L}$ ,  $M$ ,  $N$ ) was assumed to be applied on a rocket, the cause of which was exclusively the aerodynamic forces acting on the centre of pressure, and they were functions of the static margin  $x_{cp}$  (a distance between the centre of pressure and the centre of gravity), lift  $L$ , drag  $D$  and  $D_y$ , and angle of attack  $\alpha$ .

$$\vec{M} = \begin{bmatrix} \bar{L} \\ M \\ N \end{bmatrix} = \begin{bmatrix} 0 \\ -x_{cp} (L \cos \alpha + D \sin \alpha) \\ -x_{cp} D_y \end{bmatrix} \quad (11)$$

The attitude of a rocket can be determined by using the Euler angles, solving the kinematic relation below.

$$\begin{bmatrix} \dot{\phi} \\ \dot{\theta} \\ \dot{\psi} \end{bmatrix} = \begin{bmatrix} 1 & \sin \phi \tan \theta & \cos \phi \tan \theta \\ 0 & \cos \phi & -\sin \phi \\ 0 & \sin \phi \sec \theta & \cos \phi \sec \theta \end{bmatrix} \begin{bmatrix} p \\ q \\ r \end{bmatrix} \quad (12)$$

There is, however, a singular point for  $\tan \theta$  when  $\theta$  is  $90^\circ$ , which is a common occurrence in a rocket flight simulation. Thus, a quaternion equation was used instead to circumvent the singularity. The four quaternion variables were acquired by solving additional quaternion equations, detailed equations of which can be found in [50], and they were converted to Euler angles,  $\Psi$ ,  $\theta$ , and  $\phi$ , using the Euler angle-quaternion conversion equation.

These three main equations: translational motion, rotational motion, and quaternion equations, were numerically solved via a specific process. The rotational motion was first calculated to determine the angular acceleration of a rocket at the next time step after an initial condition, and then the quaternion equation was solved resulting in the Euler angles and the rocket attitude, with which the gravitational force distribution to each axis of the body fixed frame was identified. After determining the net force acting on the rocket, a translational motion was calculated, acquiring accelerations of the rocket on each axis. The three ordinary differential equations were numerically solved using the Runge Kutta 4<sup>th</sup> order method at each time step for the entire flight time. The acquired variables at the body fixed frame were then converted to variables at the Earth fixed frame using the quaternion variables. Finally, a rocket flight trajectory was drawn by integrating accelerations and then velocities for each axis of the Earth fixed frame.

The flight simulation was conducted on the basis of certain conditions and assumptions. As the NED coordinate was used as an inertial frame, it meant it was relevant to a flight problem on flat Earth (neglecting the rotation of Earth), an appropriate assumption for a sounding rocket which has a shorter flight range than that of a launch vehicle. The variation of gravitational acceleration with altitude was also neglected, which has less than a 3% error at a 100 km altitude and less than 6% at 200 km. The US standard atmospheric data was employed for air density at each altitude. The sounding rocket was assumed to have a rigid body with a constant rate of propellant consumption and to be devoid of thruster vector controlling or throttling. Although the varying drag coefficient can be numerically estimated and compared with other sources, such as OpenRocket [51] or RasAero [52]; semi-empirical data such as Missile Datcom [53]; or via a wind tunnel test, a constant value was used in this simulation, not only to achieve simplicity, but also to establish a common reference and make it easier to draw comparisons with other various rocket designs of different aerodynamic shapes. The constant drag coefficient for the simulation was 0.35 and the lift coefficient was zero.

As described earlier, this work focused on three main design parameters for a trajectory simulation. Propellant mass fraction,  $\zeta$ , was one of the three parameters, which is defined as shown in Equation (13), where  $m_p$  is propellant mass and  $m_0$  is the total mass of the vehicle.

$$\zeta = \frac{m_p}{m_0} \quad (13)$$

In this study, the term mass ratio (MR) was used to refer to the propellant fraction, the ratio of propellant to the total mass of the sounding rocket. For example, 0.7 of MR in this study meant propellant

**Table 2.** Flight simulation conditions for a single-stage rocket

Parameters	Values
Thrust	5,000 – 30,000 N
Mass ratio	0.1 – 0.7
Burn time	1 – 50 s
Specific impulse	230 s
Lift coefficient	0
Drag coefficient	0.35
Launch angle	85 degree
Static margin	1.5
Body diameter	25 – 40 cm (for 5 – 30 kN)

accounted for 70% of the total rocket mass, with 30% (dry mass) composed of the rocket systems, such as structures, payloads and any subsystem except the propellant.

For the flight simulation, the mass ratio (propellant fraction) in the range of 0.1 – 0.7 was covered. In view of the increasing use of hybrid rockets in sounding rocket flight testing, all simulated rockets had specific impulse (Isp) of 230 s, which is the typical Isp performance of a hybrid rocket. The amount of thrust simulated was in the range of 5,000 N to 35,000 N and it was a constant thrust profile for each simulation case during the burn time considered. As the diameter of a rocket's body generally increases with thrust, as shown in Fig. 1, the different thrust performance inputs in each simulation was taken into account with different rocket diameters. It was 25 cm for 5,000 N, 30 cm for 10,000 – 15,000 N, 35 cm for 20,000 – 25,000 N, and 40 cm for 30,000 N.

Burn time covered in the simulation was 50 s. The launch angle was 85 degrees and the static margin, a distance between the centre of gravity and the centre of pressure, was determined as 1.5, which is known as an appropriate value for rocket stability based on previous studies [27,54]. The flight simulation conditions are listed in Table 2. With these input variables and ranges, a flight trajectory was simulated for each different combination of these design parameters, and the peak altitudes were ascertained. For example, Fig. 2 shows the peak altitudes collected with respect to burn time and propellant fraction, MR, for a 15,000 N class single-stage sounding rocket.

## 5.0 Results and discussion

A flight simulation was conducted considering six-degree-of-freedom motion with varying amounts of thrust in the range of 5 kN – 30 kN, burn time for 50 s, and propellant fraction 0.10 – 0.70 of the total rocket mass. Through repeated flight trajectory estimations using the shooting method, reachable altitude could be established from the simulated flight data gathered. Each figure in Fig. 3 describes the variation of reachable altitude as a function of propellant fraction and burn time for a certain amount of thrust. Figure 3 (a) describes reachable altitudes and required total rocket masses using 5,000 N thrust with different propellant fractions and burn time combinations. The maximum altitudes are shown by the full line contours with each value in the unit of meter, while the dashed line contours represent the required total rocket mass with each value in kg. Clearly, with regards to a fixed burn time, a larger propellant fraction increases reachable altitude. However, for a fixed propellant fraction condition, an increased burn time does not necessarily mean a higher reachable altitude. At a certain value, burn time maximised peak altitude, once the mass ratio of a rocket was determined. For example, for a 5 kN class rocket with a propellant fraction of about 0.25, a burn time of approximately 20 s was the optimal value in terms of peak altitude, up to 10 km. For a rocket with an approximate propellant fraction of 0.37, a 28 s burn time was needed to maximise altitude reaching 20 km. Likewise, an increased propellant fraction required a longer burn time to follow the optimal design reference line in the figure, keeping

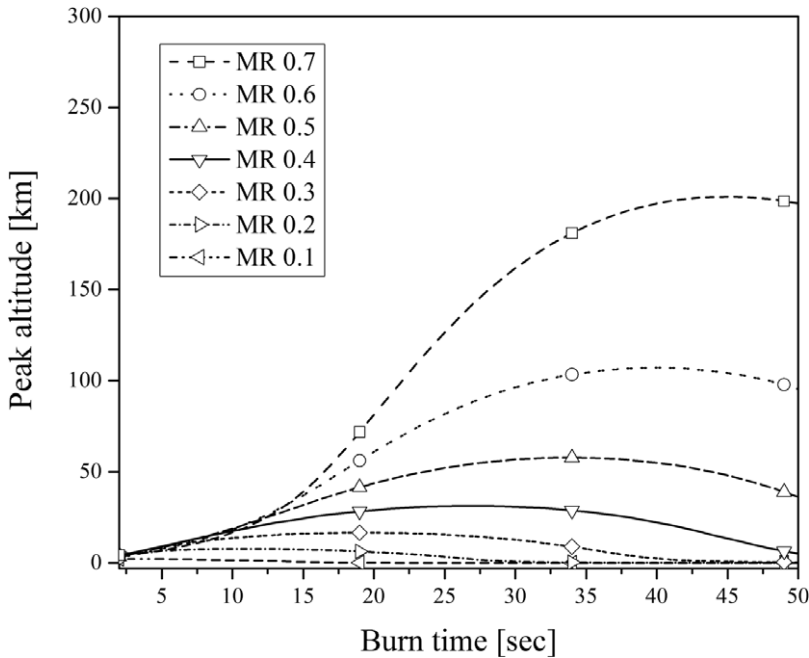


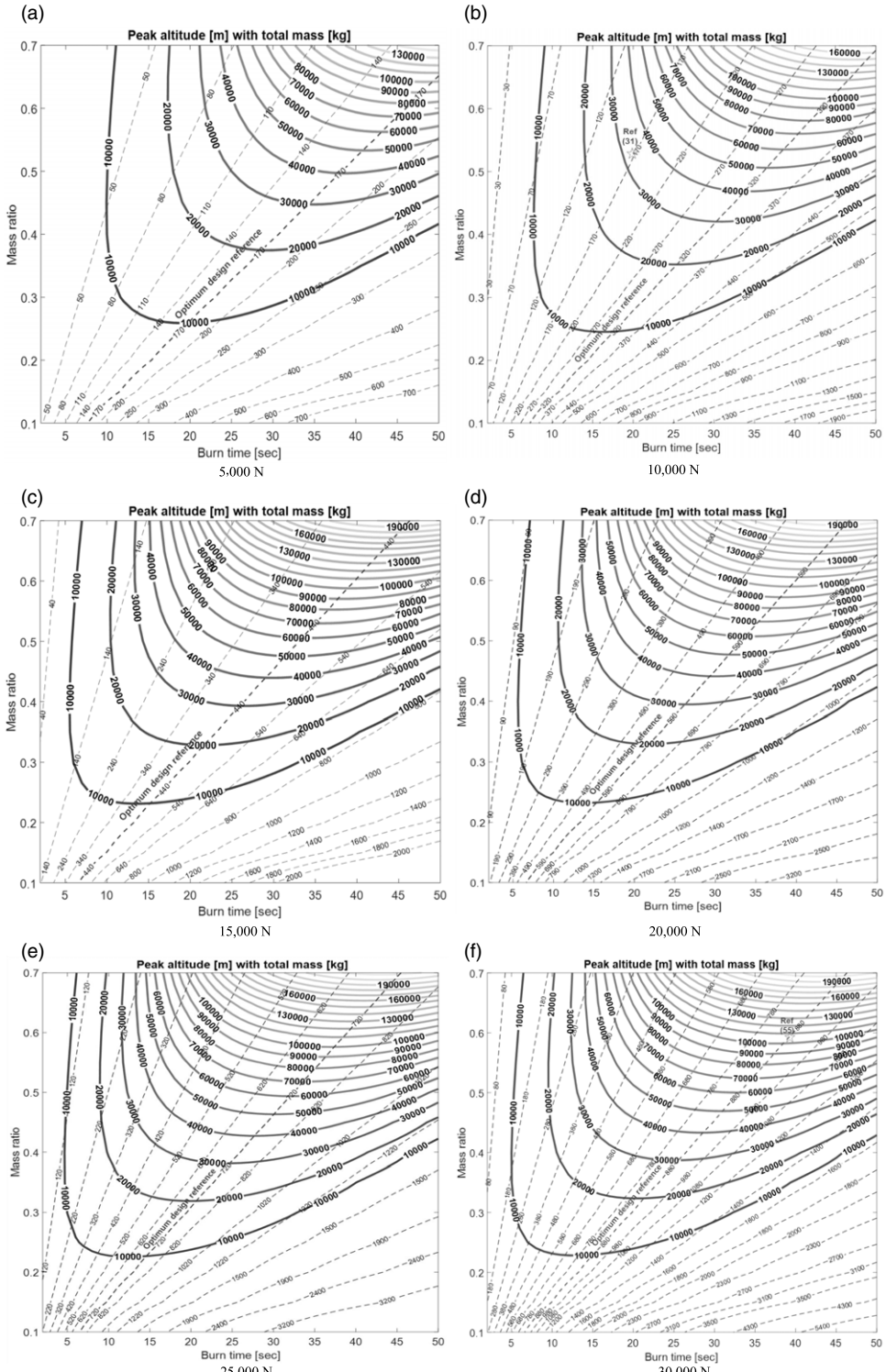
**Figure 2.** Reachable altitudes of a 15,000 N class sounding rocket with respect to burn time and mass ratio (MR, i.e. propellant fraction).

the maximised peak altitude condition at each fractional condition, interestingly with a similar required total rocket mass.

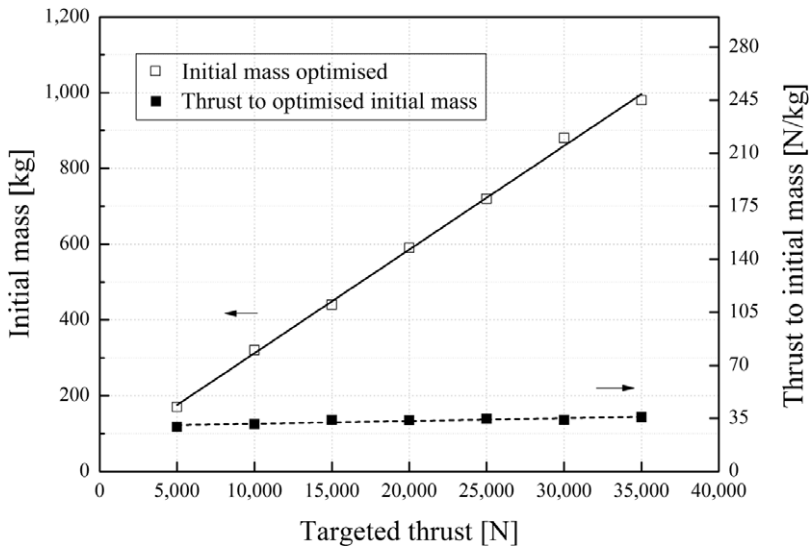
The dashed lines represent the required total rocket mass, which tends to increase with increasing burn time. This is the primary explanation for the existence of an optimal burn time for a fixed amount of thrust and propellant fraction, and for a longer burn time that does not necessarily increase peak altitude. Regardless of the mass ratio, 170 kg of total mass appears desirable for a 5 kN class rocket, when it has, as stated earlier, a specific impulse of 230 s. As shown in the other sub-figures in Fig. 3, with different thrust conditions considered up to 35 kN for the simulation, at each magnitude of thrust it exhibited a similar trend; (1) higher reachable altitude with larger propellant fraction, (2) existence of an optimal burn time for the maximum peak altitude, and (3) a certain amount of the required total mass desirable for each targeted thrust. As it was 170 kg total mass for 5 kN class, 320 kg for 10 kN, 440 kg for 15 kN, 590 kg for 20 kN, 720 kg for 25 kN, and 880 kg for 30 kN.

Figure 4 summarises these values and shows the total initial rocket mass that was optimised in terms of the maximum reachable altitude. The vertical axis on the right side is the thrust to initial mass ratio, which is proportional to the initial acceleration of the rockets. The greater the targeted thrust is, the greater the increase in optimised total mass is. The ratio of thrust to optimised initial mass remained similar, regardless of the amount of targeted thrust (approximately 35 N/kg).

As Figs. 3 and 4 are underpinned by certain conditions and assumptions, such as the flight conditions shown in Table 2, the specific values of the maximised reachable altitude with a burn time and a mass ratio may vary depending on simulation conditions. However, the results clearly indicate that a longer burning time is not necessarily desirable when maximising reachable altitude, as a greater propellant load also increases the total weight of a rocket affecting its initial acceleration, when thrust is constant. This result reinforces results from previous studies [21–23], which implied that there is a certain value for an initial acceleration that maximises the peak altitude. Moreover, augmenting this finding [21],



**Figure 3.** Single-stage sounding rocket design domains with optimal guidelines for maximum of reachable altitudes [meters] on full lines and required total masses [kg] on dashed lines, depending on the three principal design variables: Thrust (5 – 30kN), Burn time (0 – 50 s), and Mass ratio - propellant fraction (0.1 – 0.7).



**Figure 4.** Initial mass and thrust to initial mass ratio (optimised with respect to reachable altitudes) depending on the target thrust of single-stage sounding rockets with  $I_{sp}$  of 230 s.

this work also demonstrates that a prolonged powered-flight does not always lead a rocket to coast to a higher altitude. According to previous studies, a prolonged-poweredflight was beneficial only in getting over the hump of the drag curve and reaching a higher altitude. In addition, Malina et al. [21] and Ivey et al. [22] found that there was a certain initial acceleration that was most conducive to maximum altitude when thrust was constant, with a range of one to three times that of gravitational acceleration for an optimal initial acceleration, depending on the total weight of the rocket, aerodynamic drag, etc. The thrust to optimised initial mass ratio of 35 N/kg, which was recorded in this study (approximately 2.6 g), is also in line with them as it falls into the range of one to three times that of gravitational acceleration found previously.

The simulation results also made it possible to compare the experimental flight testing results. As a specific impulse of 230 s was considered in this study, it was possible to examine a hybrid sounding rocket with a similar-specific impulse performance. For example, a single-stage hybrid sounding rocket flight tested by DLR [31] has a 10 kN class thrust, 20 sec of burn time, and 0.53 propellant fraction, and it can be compared with Fig. 3 (b) from the simulation which had a 10 kN thrust. Based on this figure, a rocket with this specification is expected to reach an altitude of between 30 and 40 km, but closer to 30 km, which compares favourably with the reported experimental flight altitude of 32.3 km. These findings also reveal that if faced with similar flight conditions, the rocket with a propellant fraction of 0.53 would lack an optimal burn time, thus compromising peak altitude maximisation. It was found that a burn time of approximately 37 s is the optimal design reference, as shown in Fig. 3 (b).

Another example of a flight-tested hybrid sounding rocket with a similar specific impulse performance is Nucleus of Nammo [55]. This was a single-stage sounding rocket producing a 30 kN class thrust with a burn time of 39 s and propellant fraction of 0.59. This design condition can also be examined by comparing it with Fig. 3. The design domain suggested in Fig. 3 (f), with a 30 kN class thrust, indicates that with specifications of 0.59 MR and a 39 s of burn time, it is expected to reach an altitude higher than 100 km but lower than 110 km, suggestive of an optimal burn time of approximately 39 s. This is in accordance with the reported experimentally reached altitude by the sounding rocket of 107 km. It also recorded 39 s of firing during flight testing and it appears that the Nucleus had a favourable burn time in terms of altitude maximisation.

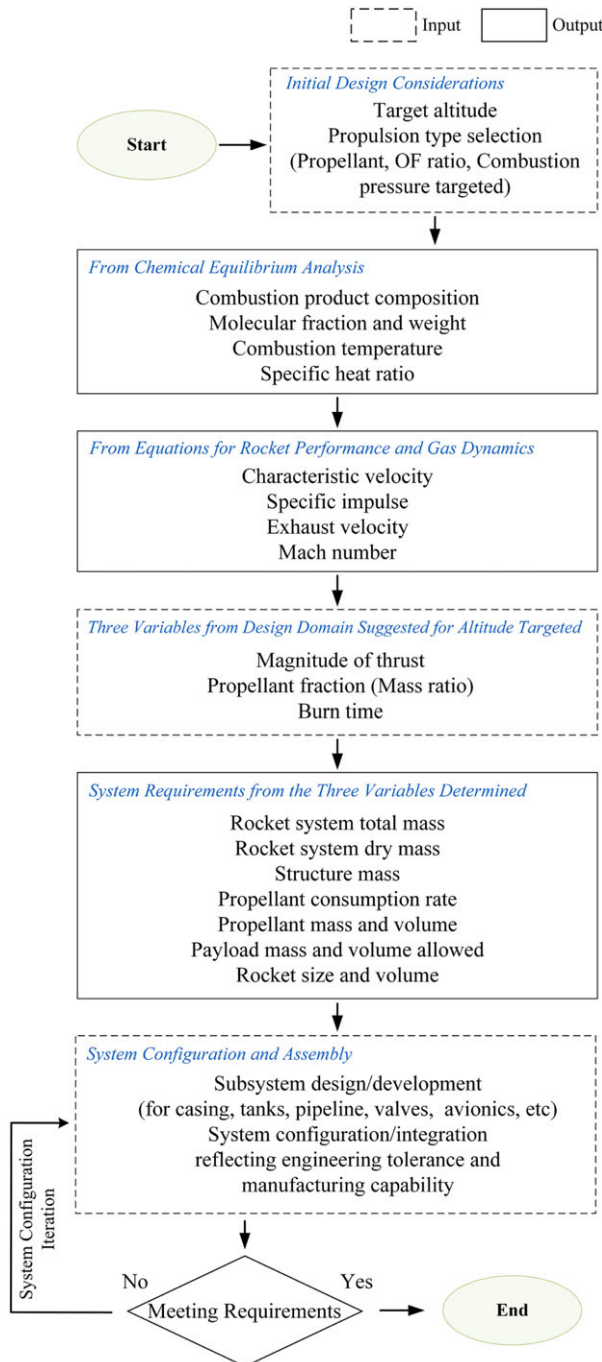


**Figure 5.** Sounding rocket design procedure suggested to reach a targeted altitude, utilising the new rocket design domain provided (Three-variable Design Method).

These new types of design domains, as shown in Fig. 3, offer clarity on the expected reachable peak altitude with respect to the design parameters considered. This result is particularly important with regards to a rocket design, as the three design inputs are among the principal parameters that can most shape the baseline of a sounding rocket design. On the basis of these observations, a new approach to

sounding rocket design has been proposed in this work, as presented in Fig. 5. The three-variable design method in this work recommends a sounding rocket design procedure, which starts from the initial design considerations, including targeted altitude, propulsion type and propulsion performance, and then determination of the three variables; magnitude of thrust, burn time and propellant fraction. This should be followed by a physical system configuration that meets the baseline determined by the three design variables. However, the design domains presented here do not necessarily imply that every design point simulated is physically feasible in a rocket system. Accordingly, before completing the design process, a specific system design and configuration and subsystems iteration is also required (depending on technological manufacturing tolerance and/or engineering constraints), with a clear understanding of their effects on flight performance in the system configuration phase.

Unlike previous optimisation studies on reachable altitude maximisation, which were arguably too theoretical or mathematical, or too specific to certain conditions and lacking sufficient consideration of design practicalities, this new design approach provides a broad and practical performance design domain. Simultaneously, these findings are conducive to a targeted and optimal reachable altitude performance and deliver an iterative system configuration and assembly with a clear understanding of their influences on output flight performance.

The specific values optimised in the design domains in this work may vary depending on specific input conditions, such as drag coefficient, lift coefficient, specific impulse performance, launch angle, etc., but the major performance trends and the design methodology verified here remain valid in other design and flight conditions too, and it is expected that they will be beneficial in understanding rocket design procedure and reaching target altitude.

## 6.0 Conclusion

With the demonstrated effect of each design input on the final altitude, a new reachable-altitude-optimised single-stage sounding rocket design procedure has been suggested utilising a new type of rocket design domain. Among the numerous sounding rocket design inputs, three major parameters were chosen and their effects on flight performance were examined. Flight simulation based parametric study was conducted in order to (a) establish the influence of the parameters on flight performance, (b) understand their effectiveness as design variables and (c) provide an optimised reference design point for the maximisation of reachable altitude. The peak altitude was examined by varying thrust, burn time and propellant fraction. In the simulation-based design parameter study, it was found that a greater propellant load on a sounding rocket (for a longer burn time) does not necessarily increase apogee altitude when thrust is constant, and that there is an optimal burn time in regard to reachable altitude maximisation. Also, regardless of burn time and mass ratio, there was an optimal initial mass for each amount of thrust targeted. With the three principal design variables—magnitude of thrust, burn time and propellant fraction—the output flight performance changed dramatically and a broad design domain was successfully devised based on the variables chosen, validating the selection of the parameters identified. The findings from the parameter study were randomly compared with experimentally flight-tested sounding rocket data, and the subsequent observations were evaluated favourably. This was also congruent with results of previous studies which had attempted to identify optimal initial acceleration. Unlike previous optimisation studies, which focused on theoretical and mathematical considerations (on occasion based on convenient assumptions), or optimisation in specific or narrow conditions without sufficient reference to the physical aspects of sounding rocket development, the three-variable design method proposed in this work is expected to confer greater practical benefits. It is also expected to be more compatible with a physical system configuration process, making it feasible to attempt an iterative system design, configuration and assembly, with a clear understanding of their effects on flight performance, even during a development process concerning an aimed peak altitude to reach.

**Acknowledgment.** This research was supported by the Basic Science Research Program through the National Research Foundation of Korea funded by the Ministry of Education (2018R1D1A1A02049748).

## References

- [1] Smart, M.K., Hass, N.E. and Paull, A. Flight data analysis of the HyShot 2 scramjet flight experiment, *AIAA J.*, 2006, **44**, (10), pp 2366–2375. doi: [10.2514/1.20661](https://doi.org/10.2514/1.20661)
- [2] Paiva, K.V., Mantelli, M.B.H. and Slongo, L.K. Experimental testing of mini heat pipes under microgravity conditions aboard a suborbital rocket, *Aerosp. Sci. Technol.*, 2015, **45**, pp 367–375. doi: [10.1016/j.ast.2015.06.004](https://doi.org/10.1016/j.ast.2015.06.004)
- [3] Lingard, J.S., Saunders, A., Merrifield, J., Caldwell, J., Longo, J. and Ferracina, L. Supersonic parachute testing using a MAXUS sounding rocket piggyback payload, 8th European Symposium on Aerothermodynamics for Space Vehicles Proceedings. European Space Agency, Lisbon, Portugal, 2015.
- [4] Florin, G., Lockowand, C. and Abrahamsson, M. Sounding rockets and stratospheric balloons, unique test platforms for re-entry systems at ESRANGE, 8th European Symposium on Aerothermodynamics for Space Vehicles Proceedings. European Space Agency, Lisbon, Portugal, 2015.
- [5] Chern, J.-S., Wu, B., Chen, Y.-S. and Wu, A.-M. Suborbital and low-thermospheric experiments using sounding rockets in Taiwan, *Acta Astronaut.*, 2012, **70**, pp 159–164. doi: [10.1016/j.actaastro.2011.07.030](https://doi.org/10.1016/j.actaastro.2011.07.030)
- [6] Boone, T.R., Shelley, E.C. and Miller, D.P. Launch cost thresholds for economic activity, *New Space*, 2018, **6**, (3), pp 201–210. doi: [10.1089/space.2017.0042](https://doi.org/10.1089/space.2017.0042)
- [7] Richardson, M.P. and Hardy, D.W.F. Economic benefits of reusable launch vehicles for space debris removal, *New Space*, 2018, **6**, (3), pp 227–237. doi: [10.1089/space.2018.0005](https://doi.org/10.1089/space.2018.0005)
- [8] Hayward, K. The Economics of Launch Vehicles: Towards a New Business Model. In *Yearbook on Space Policy*. Springer, 2017, pp. 247–256. doi: [10.1007/978-3-7091-4860-0\\_12](https://doi.org/10.1007/978-3-7091-4860-0_12)
- [9] Sarzi-Amade, N., Bauer, T.P., Wertz, J.R. and Rufier, M. *Sprite, a Very Low-Cost Launch Vehicle for Small Satellites*, Springer, 2017.
- [10] Dupont, C., Tromba, A. and Missonnier, S. Multidisciplinary system optimisation on the design of cost effective space launch vehicle, 2018, pp 3–16. doi: [10.1007/978-3-319-67988-4\\_1](https://doi.org/10.1007/978-3-319-67988-4_1)
- [11] Bae, J., Koo, J. and Yoon, Y. Development trend of low cost space launch vehicle and consideration of next generation fuel, *J. Korean Soc. Aeronaut. Space Sci.* 2017, **45**, (10), pp 855–862. doi: [10.5139/jksas.2017.45.10.855](https://doi.org/10.5139/jksas.2017.45.10.855)
- [12] Choo, K., Mun, H., Nam, S., Cha, J. and Ko, S. A survey on recovery technology for reusable space launch vehicle, *J. Korean Soc. Propuls. Eng.*, 2018, **22**, (2), pp 138–151. doi: [10.6108/kspe.2018.22.2.138](https://doi.org/10.6108/kspe.2018.22.2.138)
- [13] Goddard, R.H. A method of reaching extreme altitudes, *Smithsonian Misc. Collect.*, 1919, **71**, (2), pp. 54–57.
- [14] Tsiotras, P. and Kelley, H.J. Goddard problem with constrained time of flight, *J. Guid. Control Dyn.*, 1992, **15**, (2), pp 289–296. doi: [10.2514/3.20836](https://doi.org/10.2514/3.20836)
- [15] Tsiotras, P., Kelley, H.J. and Kelley, H.J. Drag-law effects in the goddard problem, *Automatica*, 1991, **27**, (3), pp 481–490. doi: [10.1016/0005-1098\(91\)90105-b](https://doi.org/10.1016/0005-1098(91)90105-b)
- [16] Seywald, H. and Cliff, E.M. Goddard problem in presence of a dynamic pressure limit, *J. Guid. Control Dyn.*, 1993, **16**, (4), pp 776–781. doi: [10.2514/3.21080](https://doi.org/10.2514/3.21080)
- [17] Graichen, K. and Petit, N. Solving the Goddard problem with thrust and dynamic pressure constraints using saturation functions, *IFAC Proc. Vol.*, 2008, (**41**), (2), pp 14301–14306. doi: [10.3182/20080706-5-kr-1001.02423](https://doi.org/10.3182/20080706-5-kr-1001.02423)
- [18] Bonnans, F., Martinon, P. and Trélat, E. Singular arcs in the generalized goddard’s problem, *J. Optim. Theory Appl.*, 2008, **139**, (2), pp 439–461. doi: [10.1007/s10957-008-9387-1](https://doi.org/10.1007/s10957-008-9387-1)
- [19] Munick, H. Goddard problem with bounded thrust, *AIAA J.*, 1965, (**3**), (7), pp 1283–1285. doi: [10.2514/3.3122](https://doi.org/10.2514/3.3122)
- [20] Hamel, G. Über eine mit dem Problem der Rakete Zusammenhängende Aufgabe der Variationsrechnung, *Zeitschrift für Angewandte Mathematik und Mechanik*, 1927, **7**, (6), pp 451–452.
- [21] Malina, F.J. and Smith, A.M.O. Flight analysis of the sounding rocket, *J. Aeronaut. Sci.*, 1938, (**5**), pp 199–202. doi: [10.2514/8.572](https://doi.org/10.2514/8.572)
- [22] Ivey, H.R., Bowen, J.E.N. and Oborny, L.F. Introduction to the Problem of Rocket-Powered Aircraft Performance, Vol. 1401, NACA Technical Note, USA, 1947.
- [23] Tsien, H.S. Optimum thrust programming for a sounding rocket, *J. Am. Rocket Soc.*, 1951, **21**, (5), pp 99–107. doi: [10.2514/8.4372](https://doi.org/10.2514/8.4372)
- [24] Bryson, A.E. and Ross, S.E. Optimum rocket trajectories with aerodynamic drag, *J. Jet Propuls.*, 1958, **28**, (7), pp 465–469. doi: [10.2514/8.7355](https://doi.org/10.2514/8.7355)
- [25] Garfinkel, B. A solution of the goddard problem, *J. Soc. Ind. Appl. Math. A Control*, 1963, **1**, (3), pp 349–368. doi: [10.1137/0301020](https://doi.org/10.1137/0301020)
- [26] Seywald, H. and Cliff, E.M. Optimal Rocket-Powered Ascent Study, American Control Conference. IEEE, Pittsburgh, PA, USA, 1989, pp 2026–2031.
- [27] Huh, J., Ahn, B., Kim, Y., Song, H., Yoon, H. and Kwon, S. Development of a university-based simplified H<sub>2</sub>O<sub>2</sub>/PE hybrid sounding rocket at KAIST, *Int. J. Aeronaut. Space Sci.*, 2017, **18**, (3), pp 512–521. doi: [10.5139/ijass.2017.18.3.512](https://doi.org/10.5139/ijass.2017.18.3.512)
- [28] Kobald, M., Fischer, U., Tomilin, K., Petrarolo, A., Kysela, P., Schmierer, C., Pahler, A., Gauger, J., Breitingner, J., Hertel, F. and Hochheimer, B. Sounding rocket “HEROS” - A low-cost hybrid rocket technology demonstrator, 53rd AIAA/SAE/ASEE Joint Propulsion Conference. AIAA, Atlanta, GA, USA, 2017.
- [29] Yun, Y., Huh, J., Kim, Y., Kang, S., Heo, S. and Kwon, S. Demonstration of 2,500 N-class H<sub>2</sub>O<sub>2</sub>/HDPE hybrid rocket for lab-scale sounding rocket, 2018 Joint Propulsion Conference (AIAA Propulsion and Energy Forum). AIAA, Cincinnati, Ohio, USA, 2018.
- [30] Brooks, M.J., Pitot de la Beaujardiere, J.F., Chowdhury, S.M., Genevieve, B. and Roberts, L.W. Introduction to the University of KwaZulu-Natal hybrid sounding rocket program, 46th AIAA/ASME/SAE/ASEE Joint Propulsion Conference & Exhibit. AIAA, Tennessee, USA, 2010.



- [31] Kobald, M., Fischer, U., Tomilin, K., Petrarolo, A. and Schmierer, C., Hybrid experimental rocket stuttgart: A low-cost technology demonstrator, *J. Spacecr. Rockets*, 2018, **55**, (2), pp 484–500. doi: [10.2514/1.a34035](https://doi.org/10.2514/1.a34035)
- [32] Tsohas, J., Appel, B., Rettenmaier, A., Walker, M. and Heister, S.D. Development and launch of the purdue hybrid rocket technology demonstrator, 45th AIAA/ASME/SAE/ASEE Joint Propulsion Conference & Exhibit. AIAA, Denver, Colorado, 2009.
- [33] Miklaszewski, E., Dadson, J., Fox, D., Kees, D., Larson, L., Rideout, J., Stevens, J. and Timothee, L. Pourpoint, hybrid rocket design/build/test course at Purdue University, 49th AIAA/ASME/SAE/ASEE Joint Propulsion Conference. AIAA, CA, USA, 2013.
- [34] Okninski, A. On use of hybrid rocket propulsion for suborbital vehicles, *Acta Astronaut.*, 2018, **145**, pp 1–10. doi: [10.1016/j.actaastro.2018.01.027](https://doi.org/10.1016/j.actaastro.2018.01.027)
- [35] Okninski, A., Marciniak, B., Bartkowiak, B., Kaniewski, D., Matyszewski, J., Kindracki, J. and Wolanski, P., Development of the polish small sounding rocket program, *Acta Astronautica*, 2015, **108**, pp 46–56. doi: [10.1016/j.actaastro.2014.12.001](https://doi.org/10.1016/j.actaastro.2014.12.001)
- [36] Marciniak, B., Okninski, A., Bartkowiak, B., Pakosz, M., Sobczak, K., Florczuk, W., Kaniewski, D., Matyszewski, J., Nowakowski, P., Cieslinski, D., Rarata, G., Surmacz, P., Kublik, D., Rysak, D., Smetek, J. and Wolanski, P. Development of the ILR-33 “Amber” sounding rocket for microgravity experimentation, *Aerosp. Sci. Technol.*, 2018, **73**, pp 19–31. doi: [10.1016/j.ast.2017.11.034](https://doi.org/10.1016/j.ast.2017.11.034)
- [37] Nagata, H., Ito, M., Maeda, T., Watanabe, M., Uematsu, T., Totani, T. and Kudo, I. Development of CAMUI hybrid rocket to create a market for small rocket experiments, *Acta Astronautica*, 2006, **59**, (1–5), pp 253–258. doi: [10.1016/j.actaastro.2006.02.031](https://doi.org/10.1016/j.actaastro.2006.02.031)
- [38] Faenza, M.G., Boiron, A.J., Haemmerli, B., Lennart, S., Vesterås, T. and Verberne, O. Getting ready for space: Nammo’s development of a 30 kN hybrid rocket based technology demonstrator, 7th European Conference for Aeronautics and Space Sciences. EUCASS, Milan, Italy, 2017.
- [39] Yun, Y., Seo, J., Park, K., Huh, J., Lim, J. and Kwon, S. Integration validation of key components for small sounding rockets, *Aerospace Science and Technology*, 2020, **100**, p. 105823. doi: [10.1016/j.ast.2020.105823](https://doi.org/10.1016/j.ast.2020.105823)
- [40] Tran, P.H.N., Booth, M.J., Robinson, J.H., Deyerle, L., Tarasi, N., Forster, Z. and Wirz, R. Development and Test of an Experimental Hybrid Sounding Rocket, Intercollegiate Rocket Engineering Competition (IREC). Experimental Sounding Rocket Association, Utah, USA, 2013.
- [41] Pepermans, L., Rozemeijer, M., Menting, E., Suard, N. and Khurana, S. Systematic design of a parachute recovery system for the Stratos III student built sounding rocket, 2018 Atmospheric Flight Mechanics Conference. AIAA, Georgia, USA, 2018.
- [42] Pepermans, L., Menting, E., Rozemeijer, M., Koops, B., Dahl, N.S., Suard, N., Khurana, S., van Marion, F., Kuhnert, F. and Serman, M. Comparison of various parachute deployment systems for full rocket recovery of sounding rockets, 7th European Conference for Aeronautics and Aerospace Sciences. EUCASS, Madrid, Spain, 2019.
- [43] Jung, P. History of Dauphin & Eridan Sounding Rockets, 54th International Astronautical Congress. IAC, Bremen, Germany, 2003.
- [44] Broughton, K.M., Williams, D.R., Brooks, M.J. and Pitot, J. Development of the Phoenix-1B Mk II 35 km apogee hybrid rocket, 2018 Joint Propulsion Conference (AIAA Propulsion and Energy Forum). AIAA, Cincinnati, Ohio, USA, 2018.
- [45] Chowdhury, S., Pitot de La Beaujardiere, J., Brooks, M. and Roberts, L. An integrated six degree-of-freedom trajectory simulator for hybrid sounding rockets, 49th AIAA Aerospace Sciences Meeting including the New Horizons Forum and Aerospace Exposition. AIAA, Orlando, Florida, 2011.
- [46] Christopher, N., Cojocar, T., Deery, J., Daly, M., Farrow, C., Jiang, D., Kong, S., Li, H., Liu, R., Ma, E., Marczak, M., Mihaila, A., Morrison, A., Ng, D., Paul, A., Rajkumar, V. and Yang, E. Unexploded Ordnance Hybrid Rocket, Intercollegiate Rocket Engineering Competition (IREC). Experimental Sounding Rocket Association, USA, 2018.
- [47] Arves, J., Jones, H., Kline, K., Smith, K., Slack, T., Bales, T., Arves, J., Jones, H., Kline, K., Smith, K., Slack, T. and Bales, T. Overview of Hybrid Sounding Rocket Program, 1997. doi: [10.2514/6.1997-2799](https://doi.org/10.2514/6.1997-2799)
- [48] Townsend, J.W. and Slavin, R.M. Aerobee-Hi development program, *J. Jet Propuls.*, 1957, **27**, (3), pp 263–265. doi: [10.2514/8.12711](https://doi.org/10.2514/8.12711)
- [49] Buccellato, C., Corson, B., Daniels, E., Davenport, A., Goli, M., Kapoor, R., Salbert, D., Shafer, D., Sterenberg, N. and Ticknor, R. Michigan Aeronautical Science Association Liquid Bi-Propellant Rocket, Intercollegiate Rocket Engineering Competition (IREC). Experimental Sounding Rocket Association, USA, 2018.
- [50] Yang, Y., *Spacecraft Modeling, Attitude Determination, and Control Quaternion-based Approach*, Taylor & Francis Group, LLC, 2019, Boca Raton.
- [51] Niskanen, S. Development of an open source model rocket simulation software, Masters thesis, Helsinki University of Technology, Espoo, Finland, 2009.
- [52] Rogers, C.E. and Cooper, D. Rocket aerodynamic analysis and flight simulation, Rogers Aerospace, 2011.
- [53] Burns, K.A., Deters, K.J., Stoy, S.L., Vukelich, S.R. and Blake, W.B. Missile Datcom User’s Manual, Wright Laboratory, USA, 1993.
- [54] Barrowman, J.S. Calculating the center of pressure, ESTES Vol. TIR-33, 1988.
- [55] Faenza, M., Boiron, A.J., Haemmerli, B. and Verberne, C.J. The Nammo Nucleus Launch: Norwegian Hybrid Sounding Rocket over 100km, AIAA Propulsion and Energy 2019 Forum. AIAA, IN, USA, 2019.